We are IntechOpen, the world's leading publisher of Open Access books
Built by scientists, for scientists

4,800
Open access books available

122,000
International authors and editors

135M
Downloads

Our authors are among the

154
Countries delivered to

TOP 1%
most cited scientists

12.2%
Contributors from top 500 universities

CLARIVATE ANALYTICS
BOOK CITATION INDEX
INDEXED

WEB OF SCIENCE™

Selection of our books indexed in the Book Citation Index in Web of Science™ Core Collection (BKCI)

Interested in publishing with us?
Contact book.department@intechopen.com

Numbers displayed above are based on latest data collected.
For more information visit www.intechopen.com

10

Crystallization of Sub-Micrometer Sized ZSM-5 Zeolites in SDA-Free Systems

Nan Ren[1,*], Boris Subotić[2] and Josip Bronić[2]
[1]*Department of Chemistry, Shanghai Key Laboratory of Molecular Catalysis and Innovative Materials and Laboratory of Advanced Materials, Fudan University, Shanghai*
[2]*Ruđer Bošković Institute, Division of Materials Chemistry, Laboratory for the Synthesis of New Materials Zagreb*
[1]*People's Republic of China*
[2]*Croatia*

1. Introduction

In recent years, the threat of the potential shortage of oil becomes one of the difficult problems which not only influences the quality of human life but also triggers the regional conflicts or wars. Thus, the oil management becomes the hottest topic in the contemporary economical and political world. To well solve that problem, there are two different approaches, 1) to discover/develop the alternative energy sources such as: bio-energy (biogas, biofuel), sunlight energy (or power plants), energy of wind (or power plants), nuclear energy (or power plants), etc. and 2) to increase the efficiency of crude oil (fossil fuels) processing and quality of final product. Although the first one seems interesting and ambitious, the existing drawbacks such as the low (but increasing) efficiency of sunlight transformation and the potential risk of the leakage of radioactive materials from nuclear facilities, become the great obstacle for the fast and promising development of these types of 'New plants Energetic Strategy'. Compare with the first approach, the latter seems more mild, reliable and realizable. To achieve such goal, the increase of the efficiency of catalysts is the key. Most frequently, different types of zeolites are used as catalysts for crude oil processing – among them, zeolite ZSM-5 has most expressive role.

Zeolite ZSM-5, as a member of the family of pentasil zeolites, has aroused tremendous interest after its first discovery by the research group of Mobile Company in the year 1972 [1]. With its adjustable framework Al content (from 0 to about 8Al per unit cell), two dimensional micropore channels (0.55 nm × 0.54 nm; Fig. 1a), sinusoidal pore geometry along c axis (Fig.1b) and easy insertion of hetero-T atoms, this material plays an important role in many of crucial catalytic processes such as hydro-cracking, de-waxing, alkylation, etc., [2-5] as well as in separation of organic compounds with different sizes and shapes [6]. In the case when zeolite ZSM-5 was used as catalyst, most of reactions are 'diffusion-controlled' [7]. This means that the product distribution largely depend on the nature and location of active sites in the crystalline framework of catalyst. Thus, the increase of the

* Corresponding Author

catalyst reactivity and thus, its efficiency can be achieved by increase of easily accessible active sites and by decrease of the length of diffusion path of reactants/intermediates/products and eliminating the probability of the occurrence of coke-formation side-reactions. Upon decreasing the crystal size, the diffusion paths of the reactant and product molecules inside the pores becomes shorter, and thus this can result in the reduction or elimination of undesired diffusion limitations of the reaction rate [8-10].

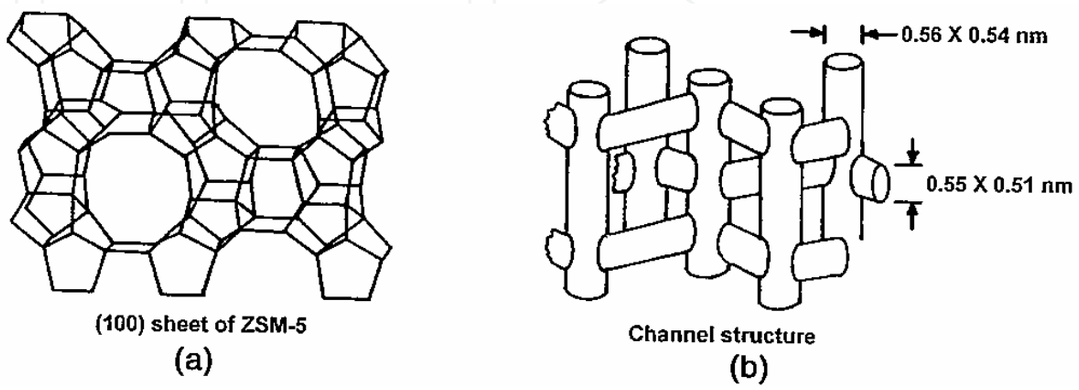

Fig. 1. The topological view of ZSM-5 crystals, (a) skeletal diagram of the (100) face and (b) channel structure.

To synthesize small-sized ZSM-5 zeolites and achieve the precise control of crystal size, the synthesis mechanism of ZSM-5 and the critical processes occurring during its crystallization should be understood thoroughly. From the well documented literature data, it is evident that, besides the framework constituents such as silica and alumina in different forms [1,11-18] and different alkaline bearing cations [13,19-24], the presence of organic structure directing agent (SDA) is vital for the synthesis of zeolite ZSM-5 [1,11-13,15,18,21,25] and other high-silica types of zeolites.

Zeolite ZSM-5 is conventionally synthesized by hydrothermal treatment of the reactive gel containing aluminosilicate as well as the tetrapropylammonium ions (TPA^+) as structure directing agent [1,11-13,15,18,25-27]. For the sake of industrial scale production, the synthesis of ZSM-5 zeolites could also be performed by using cheaper silica sources (fumed or precipitated silica) with reduced amount of SDAs. In such cases, the starting reaction mixture appears in the form of dense gel and the gelation phenomena can be observed at very short period of the mixing of the reactants; such system is also denoted as heterogeneous crystallization system [28,29]. However, the size of the products obtained from this route is normally in the range of several micrometers to tens micrometers, and the crystal size seems very difficult to be adjusted.

Using the known gel compositions for the synthesis of ZSM-5 zeolites, recently, a method called 'clear solution' synthesis has been proposed for the successful preparation of small sized ZSM-5 zeolites [30]. Since the 'clear solution' approach generally uses silica species in molecular form and thus a transparent solution appears at the initial stage of crystallization, such synthesis system is also called homogeneous crystallization system [28,29]. Although the crystal size could be facilely controlled by this method, such approach has obvious drawbacks such as low product yield (less than 5 wt. %), use of large amount of both SDAs

(SDA/SiO_2 ratio normally exceeds 0.2) and expensive silica sources (normally TEOS), which inevitably increases the production cost [31].

Thus, an expected ideal approach for the synthesis of small sized ZSM-5 zeolites is a compromise between heterogeneous and homogeneous crystallization systems. However, even in the case of successful compromise between heterogeneous and homogeneous crystallization systems, the problem of use of SDAs is still persisting [27, 32-36]. On the other hand, many attempts of the synthesis of zeolite ZSM-5 without organic templates [6,25,27,34-49] were encountered with another group of problems such as that zeolite ZSM-5 can be synthesized only in narrow ranges of SiO_2/Al_2O_2 (~ 40-70) and Na_2O/SiO_2 (~ 0.13-0.20) [36], formation of impurity phases such as un-reacted amorphous solids [47], quartz [41], mordenite [42] and analcime [44], uncontrollable crystal size [25], long crystallization time [40] and low yield [40].

Most of the mentioned problems can, however, be overcome by addition of small amount of seed crystals (ZSM-5, silicalite-1) in the TPA^+-free reaction mixture [6, 27, 35, 38, 40, 45, 50]. Seed induction synthesis is a well developed strategy which could not only shorten the duration of synthesis, but also control the product properties [51]; addition of seed crystals results in the formation of zeolite ZSM-5 with high degree of crystallinity and a narrow size distribution at short synthesis times [38,40]. Such method has been used for the synthesis of zeolites with various framework topologies [52]. Recently, small sized zeolites were obtained fastly, using this approach [53]. This method, although old, is still under developing.

Taking into consideration the background of ZSM-5 synthesis conditions, and accompanying this with the basic knowledge of seed induced synthesis, we have developed a seed surface crystallization (SSC) approach, in which the sub-micrometer sized ZSM-5 zeolites can be obtained in a controllable manner [50, 54, 55]. More importantly, the growth of crystalline end products is achieved in a heterogeneous, SDA-free crystallization system, which is good basis for their further industrial-scale production and use in various applications.

In this chapter, SDA-free, SSC approach for the crystallization of sub-micrometer sized ZSM-5 zeolites including the influence of various synthesis parameters on the product properties and the crystallization mechanism will be discussed in detail. The relevant content is divided into five parts: (1) Controllable synthesis, (2) Influence of batch alkalinity, (3) Influence of sodium ions and gel ageing, (4) Crystallization mechanism, and (5) Modeling approach.

2. Controllable synthesis of sub-micrometer sized ZSM-5 zeolites

Batch oxide molar chemical composition of the reaction mixture (hydrogel) for the synthesis was 1.0 Al_2O_3/100 SiO_2/28 Na_2O/4000 H_2O. A series of silicalite-1 nanocrystals having different mean diameters (90, 180, 220, 260 and 690 nm; Fig. 2) were prepared by synthesis from clear solution and used as seeds for the further growth of ZSM-5 nanocrystals.

Fig. 3 shows that the well crystalline ZSM-5 crystals are obtained after 2 h of hydrothermal treatment at 483K with addition of 4 wt.% of seeds (with respect to the total amount of silica in the reaction mixture). The crystal size of product increases with increasing size of seed crystals as can be seen in the corresponding SEM images (Fig. 4).

On the other hand, using different amount of the same seed crystals (260 nm in this case), the crystal size of the product decreases with increasing amount of added seed crystals (Fig. 5).

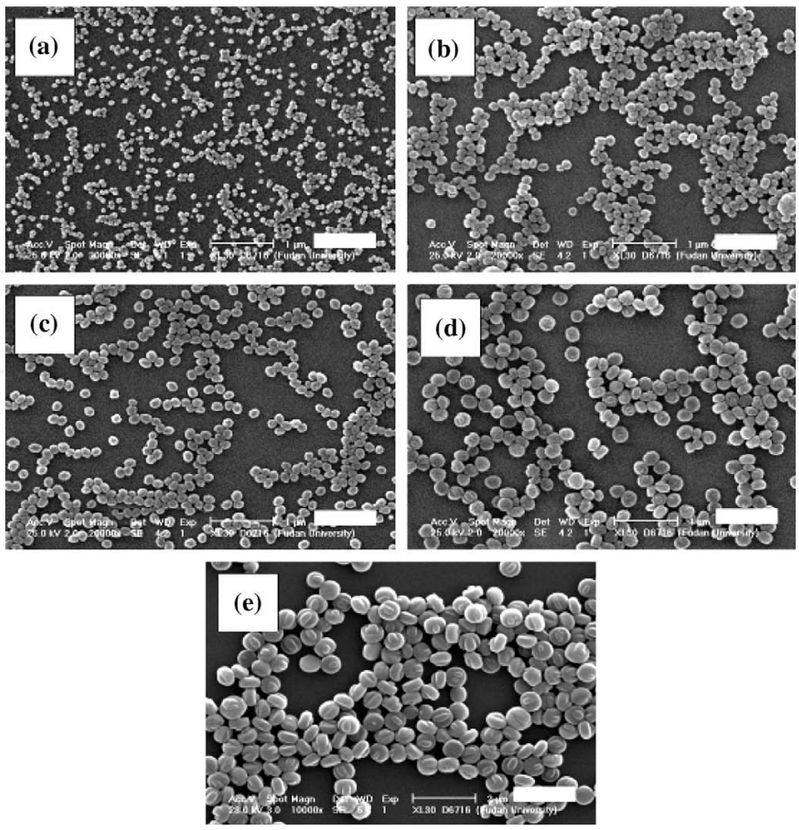

Fig. 2. SEM images of silicalite-1 nanocrystals with diameters of 90 (a), 180 (b), 220 (c), 260 (d), and 690 nm (e). The scale bars in a-d are of 1 μm, and of 2 μm in e. (Adopted from Ref. [50] with permission of Publisher.)

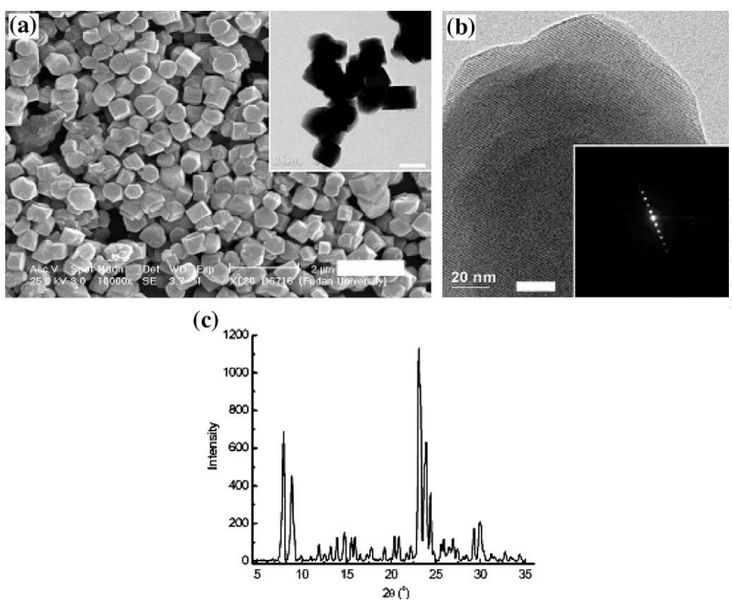

Fig. 3. The SEM (a), TEM (inset of a), High magnification TEM images (b), electron diffraction (ED) pattern (inset of b) and XRD pattern of ZSM-5, synthesized using 4 wt. % of

seed (260 nmsilicalite-1 crystals). The scale bars are of 2 μm in (a) and 20 nm in (b). (Adopted from Ref. [50] with permission of Publisher.)

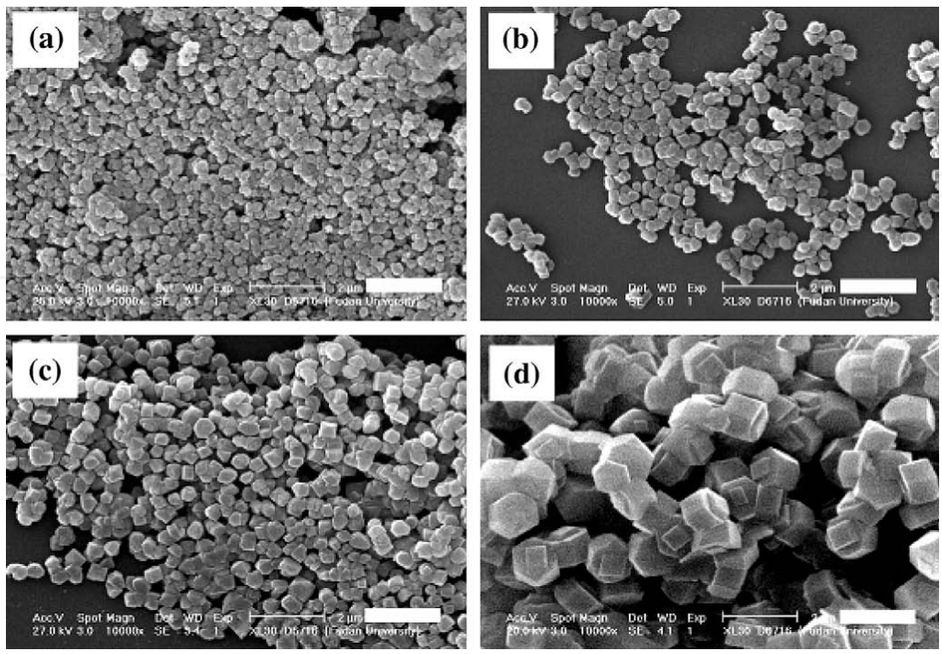

Fig. 4. SEM images of ZSM-5 samples synthesized with using 4 wt. % of: 90 nm (a), 180 nm (b), 220 nm (c) and 690 nm (d) silicalite-1 seed crystals. The scale bars in all the images are of 2 μm. (Adopted from Ref. [50] with permission of Publisher.)

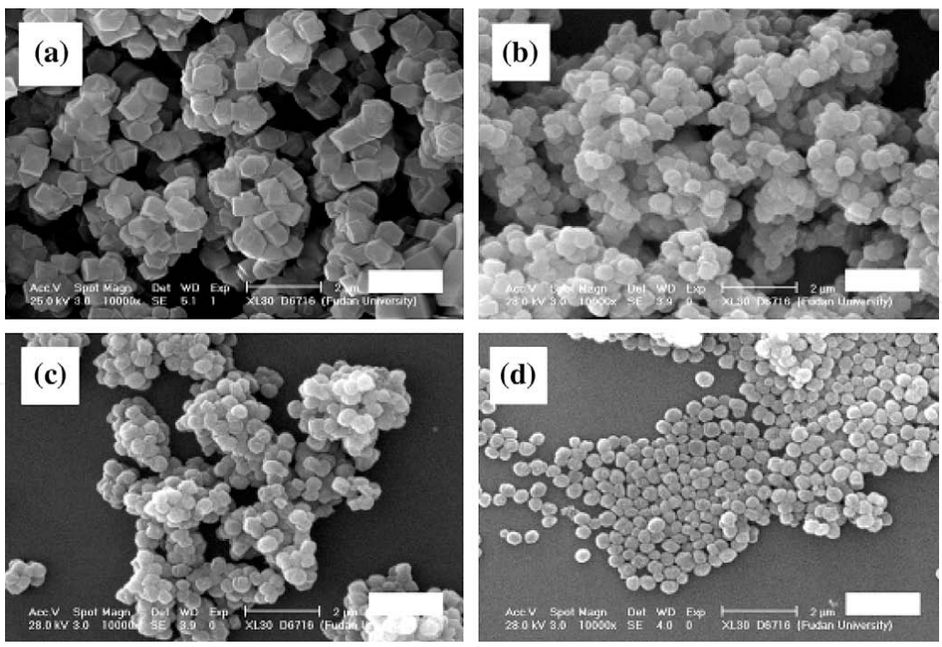

Fig. 5. SEM images of ZSM-5 samples synthesized by using 4 (a), 8 (b), 16 (c) and 32 (d) wt. % of 260 nm silicalite-1 seed crystals. The scale bars in all the images are of 2 μm. (Adopted from Ref. [50] with permission of Publisher.)

All the products are entirely crystalline and have adjustable size in the range from 270 nm to 1100 nm. This indicates that the SSC approach is a powerful tool for controlling the crystal size of the ZSM-5 zeolites. Besides the crystal size, the morphology of the product could also be controlled via changing the morphology of the seed crystals. The surface-stacking morphology of the silicalite-1 seed crystals (synthesized via microwave heating method) could be fairly well 'cloned' to the final ZSM-5 products (Figure 6). Based on the above phenomena, it could be found that the product properties could be adjusted via a 'seed-dependent' manner.

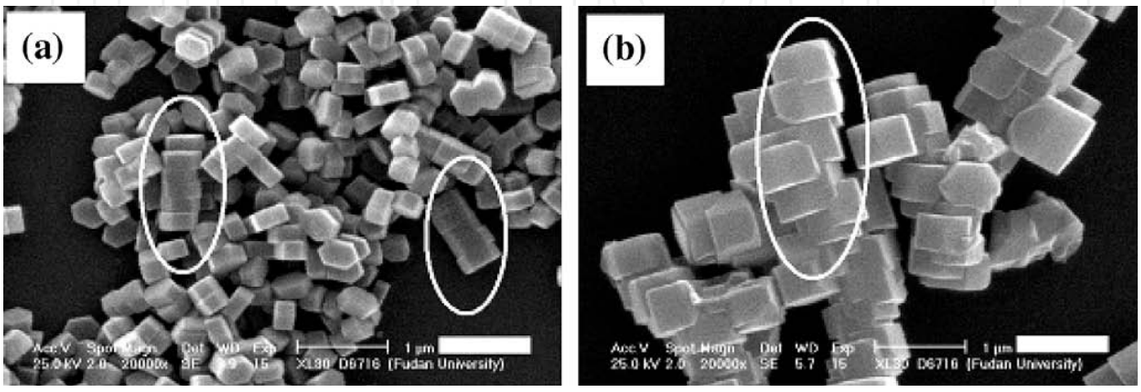

Fig. 6. The silicalite-1 seed crystals with surface-stacking morphology (a) and the corresponding ZSM-5 product (b). The scale bars is of 1 μm. (Adopted from Ref. [50] with permission of Publisher.)

3. Influence of batch alkalinity

Although the controllability of SSC approach has been proved by successful syntheses of sub-micrometer sized ZSM-5 zeolites by using different kinds of silicalite-1 seed crystals, another interesting aspect of this investigation is a study of the critical processes which occur during the crystallization. The materials with more controllable functionalities may be synthesized only with the thorough understanding of the crystallization mechanisms. In order to achieve this goal, the parameters influencing the crystallization pathway and properties of the products are adjusted. Since it is well known that the batch alkalinity play the key role in zeolite synthesis [13, 22, 30, 56-58], the influence of batch alkalinity, $A=[Na_2O/SiO_2]_b$, of this SDA-free system, is in detail studied in this part. In this part of study, the reaction mixtures (hydrogels) having different batch alkalinities, A, were seeded with 4 wt. % of 260 nm silicalite-1 seed crystals. The samples were characterized by SEM, XRD and PSD analyzes.

Fig. 7 shows the SEM images of the crystalline end products (zeolite ZSM-5) synthesized at different batch alkalinities. It can be clearly observed that at low batch alkalinities ($A \leq 0.003$), the ZSM-5 crystals are either surrounded or covered with amorphous species, indicating that the crystallization process is not completed. Increase of the batch alkalinity causes the morphological change of the samples from irregular particles ($0.004 \leq A \leq 0.005$) to cubic crystals ($0.006 \leq A \leq 0.010$). With further increase of the batch alkalinity ($0.011 \leq A \leq 0.012$), the morphologies of the samples again return to irregular shapes.

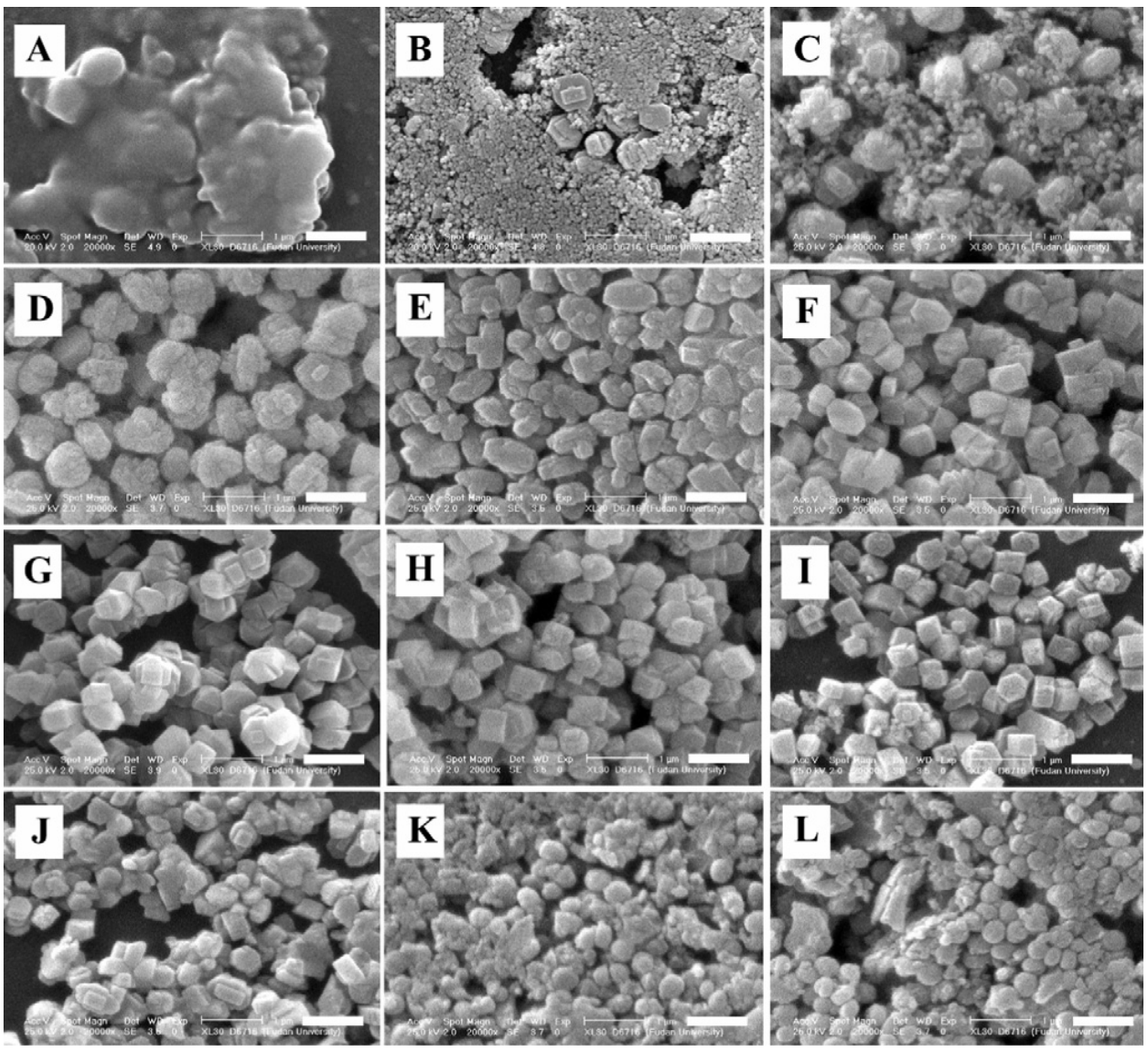

Fig. 7. SEM images of the products hydrothermally synthesized (at 438 K for 2 h) from the reaction mixtures (hydrogels) having: A = 0.001 (A), A= 0.002 (B), A = 0.003 (C), A = 0.004 (D), A = 0.005 (E), A = 0.006 (F), A = 0.007 (G), A = 0.008 (H), A = 0.009 (I), A = 0.010 (J), A = 0.011 (K), and A = 0.012 (L). The scale bars in all figures are of 1 μm.
(Adapted from Ref. [54] with permission of Publisher)

XRD analysis of the products revealed that fully crystalline zeolite ZSM-5 are obtained within the alkalinity range of $0.006 \leq A \leq 0.010$, which is in accordance with the observation in the corresponding SEM images (Figs. 7F – 7L).

In order to find more details of particulate properties, the Laser Light Scattering analysis of the obtained samples has been carried out. The particle size distribution (PSD) curves of the samples, measured by Mastersizer 2000 (Malvern) particle size analyzer, are shown in Fig. 8. The crystalline end products obtained under optimal alkalinity range ($0.006 \leq A \leq 0.01$) appear as a mixture of single crystals (50 – 60 % by number) having the size between 400

and 600 nm and aggregates of the single particles (40 – 50 % by number) having the size higher than 600 nm.

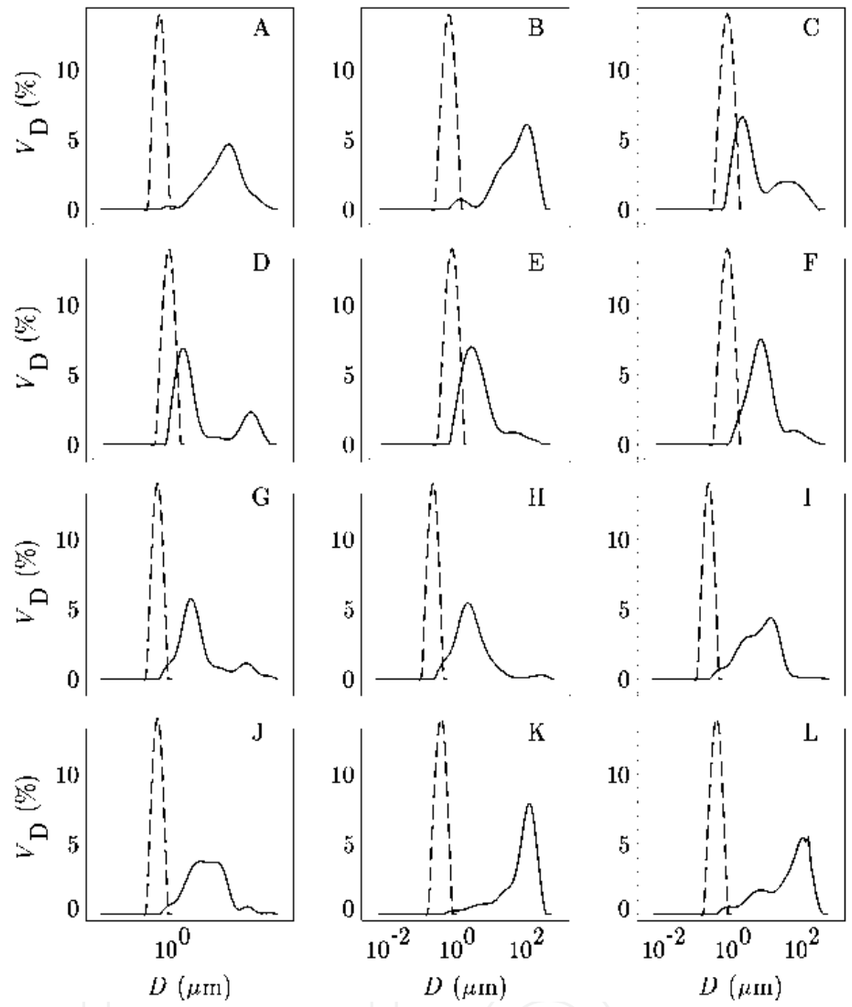

Fig. 8. Particle size distribution (by volume) of the products hydrothermally synthesized (at 438 K for 2 h) from the reaction mixtures (hydrogels) having: A = 0.001 (A), A = 0.002 (B), A = 0.003 (C), A = 0.004 (D), A = 0.005 (E), A = 0.006 (F), A = 0.007 (G), A = 0.008 (H), A = 0.009 (I), A = 0.010 (J), A = 0.011 (K), and A = 0.012 (L). Dashed curves represent the particle size distribution of silicalite-1 nanocrystals. V_D is volume percentage of crystals having the sphere equivalent diameter D. (Adopted from Ref. [54] with permission of Publisher)

Besides the phase purity and particulate properties, the Si/Al ratio of final products also correlates very well with the batch alkalinity. Table 1 summarizes the influence of alkalinity on the product properties. It could be concluded that the well crystallized ZSM-5 zeolites with adjustable Si/Al ratio from 10 - 18 can be obtained in the alkalinity range of $0.006 \leq A \leq 0.010$.

Batch alkalinity[a]	Phase[b]	Si/Al ratio[c]	Particle shape[d]
0.001	Amor[e]+ZSM-5	47	*f*
0.002	Amor[e]+ZSM-5	43	*f*
0.003	Amor[e]+ZSM-5	32	irregular
0.004	ZSM-5	28	irregular
0.005	ZSM-5	23	irregular+cubic
0.006	ZSM-5	18	cubic
0.007	ZSM-5	15	cubic
0.008	ZSM-5	12	cubic
0.009	ZSM-5	10	cubic
0.010	ZSM-5	9	cubic
0.011	Phillipsite+ZSM-5 +Amor[e]	11	Spherical+irregular
0.012	Phillipsite+ZSM-5 +Amor[e]	11	Spherical+irregular

a. $A=[Na_2O/H_2O]_b$
b. Determined from corresponding XRD patterns
c. Calculated from XRF results
d. Obtained from SEM observations
e. Amor, abbreviation of amorphous
f. Exact information cannot be provided because of the existence of large portion of amorphous impurities
(Adopted from Ref. [54] with permission of Publisher)

Table 1. Summary of structural, chemical and morphological properties of the products obtained at different alkalinities

4. Influence of sodium ions and gel ageing

It is expected that, besides the influence of alkalinity, sodium ions [13, 22, 56-58] and duration of room-temperature gel ageing [59] also influence the crystallization pathway and properties of zeolite ZSM-5. The sodium ion is recognized as the potential template ions which make the influences on the nucleation process of MFI zeolites especially in the SDA-free system [13, 22, 57, 58].

On the other hand, room temperature ageing of the reaction mixture shortens not only the duration of 'induction period' and the entire crystallization process, but also diminishes the differences in crystal size distributions of the final product [59, 60]. Moreover, in some cases, the ageing of the reaction mixture (hydrogel) influences also the morphology [61] and even phase composition of the final product [62]. From the above reasons, the influences of the mentioned parameters on the properties of crystallized zeolite ZSM-5 are described in this part. Since the increase of batch alkalinity ($A=[Na_2O/H_2O]_b$) is accompanied with the increase of sodium content, the related studies are performed at different batch alkalinities with the addition of sodium sulphate as the source of sodium ions excess. The batch content of sodium ions is expressed as $B = [Na^+/SiO_2]_b$. The batch molar composition of the reaction mixture for the synthesis of zeolite ZSM-5 is expressed as, $1.0Al_2O_3/100SiO_2/xNa_2O/4000H_2O/yNa_2SO_4$, where the values x and y are changed to adjust the batch alkalinity and batch content of sodium ions, respectively. The samples synthesized at different alkalinity and different sodium ion content are denoted as A/B (e.g., 0.003/0.24 for A = 0.003 and B = 0.24).

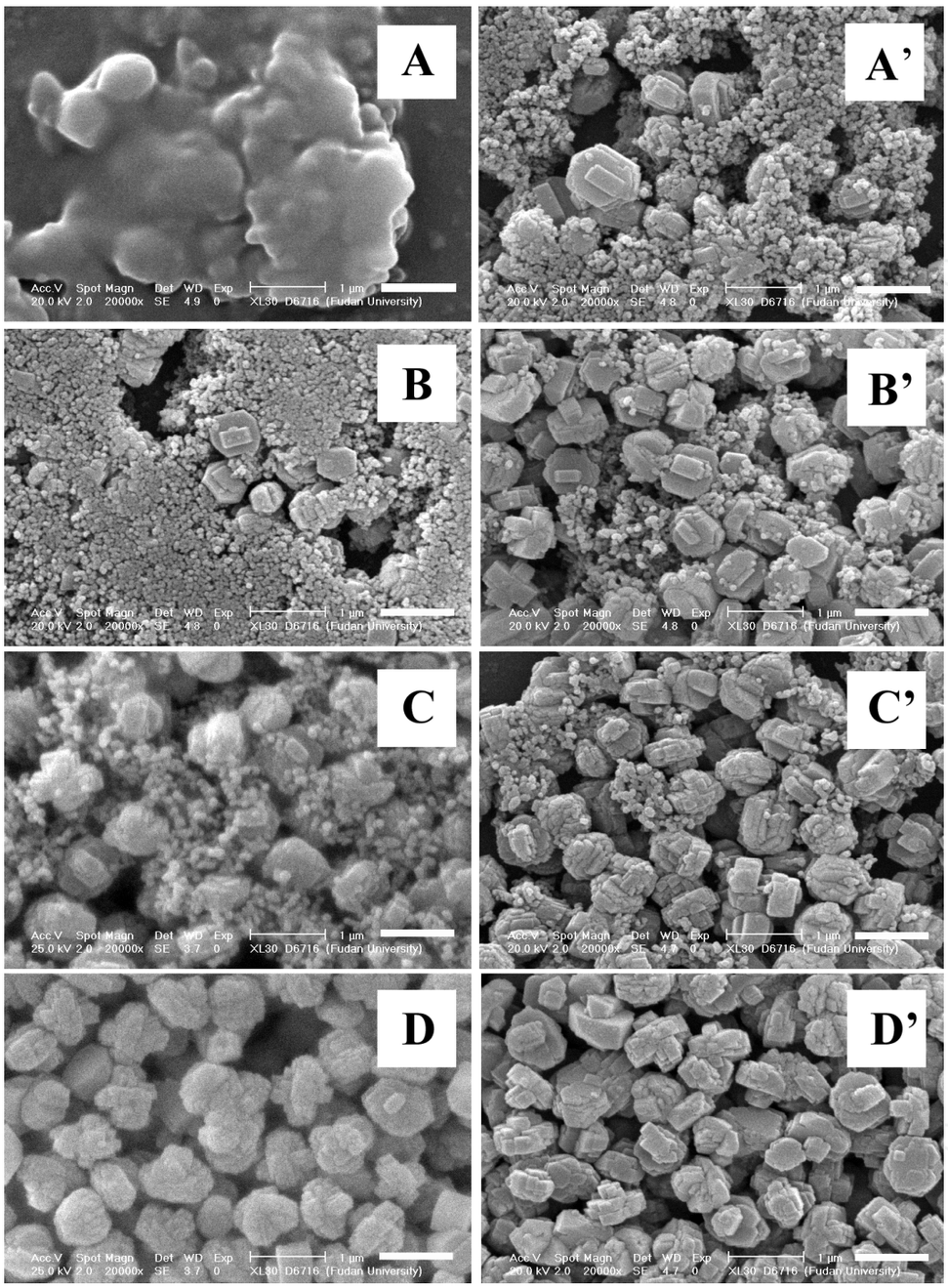

Fig. 9. SEM images of the products obtained by hydrothermal treatment (at 483 K for 2 h) of the reaction mixtures 0.001/0.08 (A), 0.001/0.64 (A'), 0.002/0.16 (B), 0.002/0.64 (B'), 0.003/0.24 (C), 0.003/0.64 (C'), 0.004/0.32 (D) and 0.004/0.64 (D'). The scale bars are of 1 μm. (Adopted and reproduced from Ref. [55] with permission of Publisher)

Fig. 9 shows the SEM images of the product obtained by hydrothermal treatment (at 483K for 2h) of the reaction mixtures having low alkalinities (A = 0.001 - 0.004) and different batch contents of sodium ions (B = 0.08 and 0.64). It can be observed that the increase of the batch content, B, of sodium ions at the same batch alkalinity, A, does not significantly influence the

morphology of the final product, as can be seen comparing of the samples prepared without (Figs. 9A, 9B, 9C and 9D) and with addition of sodium sulphate (Figs. 9A′, 9B′, 9C′ and 9D′). Also, the addition of sodium sulphate in the reaction mixture does not affect the phase composition (crystallinity) of products as revealed by XRD analysis of the product samples.

Knowing the templating role of sodium ions in the TPA-free synthesis of MFI-type zeolites [13, 22, 56-58], these findings indicate that the rate-determining factor is concentration of "free" low-molecular weight silicate species, in the short synthesis duration of this seed-induction system

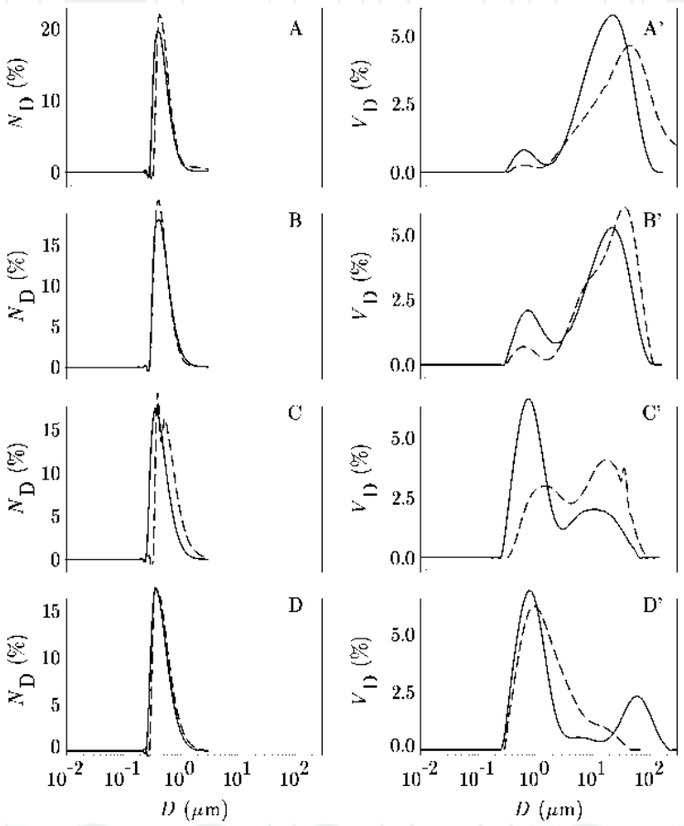

Fig. 10. Particle size distributions by number (A, B, C and D) and by volume (A′, B′, C′ and D′) of the products obtained from reaction mixtures having two batch content (B = $[Na^+/SiO_2]_b$) of Na ions 0.08 (dashed curves) 0.64 (solid curves). Alkalinity (A = $[Na_2O/H_2O]_b$) were: 0.001 for A and A′, 0.002 for B and B′, 0.002 for B and B′, 0.003 for C and C′, 0.003 for C and C′, 0.004 for D and D′. N_D is number percentage and V_D is volume percentage of crystals having the sphere equivalent diameter D. (Adopted from Ref. [55] with permission of Publisher)

Since the generation of these species is mainly caused by hydrolysis of silica precursors which depend on the concentration of "free" OH^- ions and thus, on the batch alkalinity, A [54], it is evident that the alkalinity of system, A, determines the rate of crystallization and not the concentration of "free" Na^+ ions. In the other words, when A < 0.004, fully crystalline product cannot be obtained for $t_c \leq 2$ h regardless to the content of sodium ions in the reaction mixture [54,55].

Fig. 10 shows that the fraction of the small single particles (ZSM-5 crystals formed by growth of silicalite-1 seed crystals) having the size 400 – 600 nm increases with increasing alkalinity, *A*, of the reaction mixture and that, for a given batch alkalinity, the fraction of the single 400 – 600 nm particles increases with increasing value of *B*.

According to the principals of aggregation of zeolite particles, the tendency to aggregation decreases with the increase of the (negative) crystal surface charge (repulsion effect), and increases with the increase of the concentration of the "compensating" Na^+ ions [55]. It is evident that at the simultaneous increase of OH^- ions and Na^+ ions with increasing alkalinity, *A*, the repulsive force prevails the "compensating" effect of Na^+ ions. In this context, addition of sodium sulfate additionally increases the negative charge of the crystal surface by oxy-anion effect of SO_4^{2-} ions [63] and, at the same time, additionally reduces the "compensating" effect of Na^+ ions. The result is that the aggregation is considerably reduced in the presence of sodium sulphate.

When the batch alkalinity further increases to A = 0.007, the perfect small-sized ZSM-5 crystals can be obtained, as described in previous section. An increase of the batch amount of sodium ions does not influence the phase purity of products as it was revealed by XRD analysis of the samples. However, the surface of the crystals become rough as it can be observed in the corresponding SEM images (Fig. 11). This phenomenon could be attributed to the effect of sodium ions on the cross-linking and polymerization of the silicate species in solution [64]; the species formed by cross-linking and polymerization are further deposited onto the crystalline surface of the final crystals, causing the roughing of the surface morphology of the product. This assumption is further supported by the increase of Si/Al ratio of the crystalline end product from 15 for $[Na^+/SiO_2]_b$ = 0.56 to 20 for $[Na^+/SiO_2]_b$ = 1.0 and simultaneous decrease of Si concentration in the liquid phase of the reaction mixture from 20.23 mg/ml for $[Na^+/SiO_2]_b$ = 0.56 to 14.00 mg/ml for $[Na^+/SiO_2]_b$ = 1.0, accompanying with the increase of the solid recovery yield from 42% to 50%. The surface roughing phenomena caused by the deposition of active species from liquid to solid phase (crystals) can also be evidenced by the increase of the average size of the crystalline end products (see PSD curves in Fig. 12). More interestingly, the particle size distribution also becomes narrower with the increased amount of sodium ions. This indicates that the addition of sodium sulphate into reaction mixture also prevents aggregation of the ZSM-5 crystals formed during hydrothermal treatment as was already shown in the cases of low batch alkalinities.

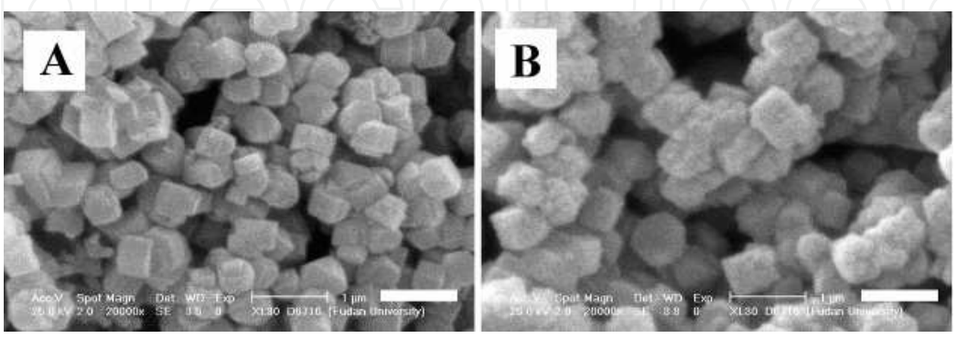

Fig. 11. SEM images of the products obtained by hydrothermal treatment (at 483 K for 2 h) of the reaction mixtures 0.007/0.56 (A) and 0.007/1.0 (B). The scale bars are of 1 μm. (Adopted from Ref. [55] with permission of Publisher)

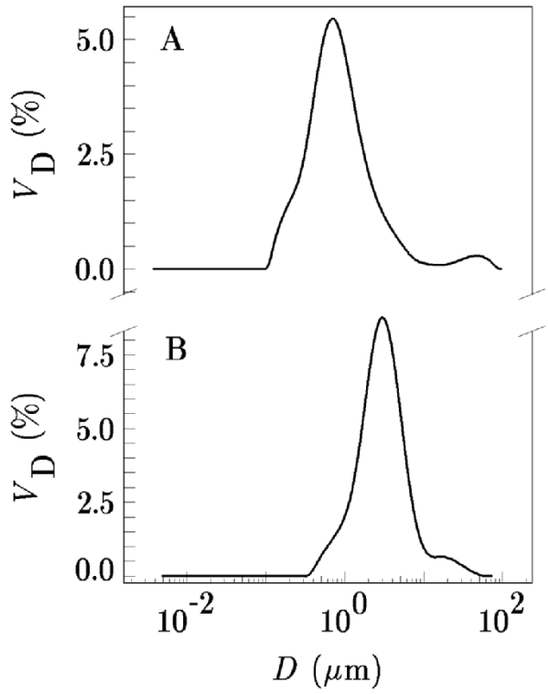

Fig. 12. Particle size distributions by volume of the products obtained by hydrothermal treatment (at 483 K for 2 h) of the reaction mixtures 0.007/0.56 (A) and 0.007/1.0 (B). (Adopted from Ref. [55] with permission of Publisher)

From the above results, it could be concluded that the addition of excess amount of sodium ions into the crystallization system has apparent effect on the particulate properties of the product. At low batch alkalinity, the additional sodium ions causes de-aggregation of the final products, rendering the particles with more uniform size distributions. At high batch alkalinity, the excess amount of sodium ions triggers the surface condensation reactions on the crystalline end products. However, the crystallization rate is not enhanced by the increase of batch sodium ion content, indicating that the determining factor of crystallization of ZSM-5 zeolites in SDA-free system is concentration of low molecular weight silicate species, determined by batch alkalinity.

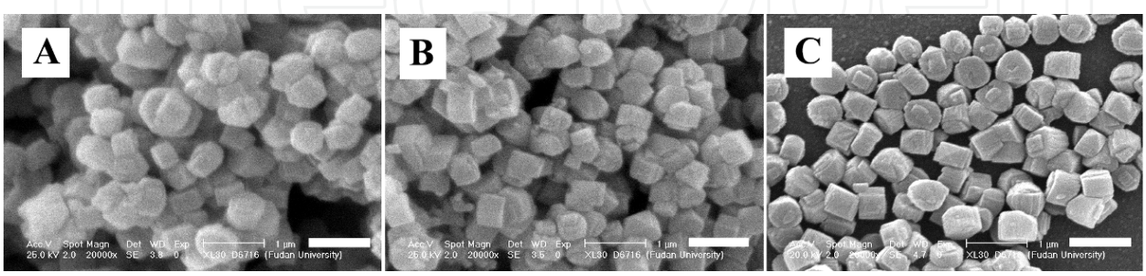

Fig. 13. SEM images of the products obtained by hydrothermal treatment (at 483 K for 2 h) of the reaction mixtures aged at room temperature for 0 (A), 3 (B) and 48 h (C) in the presence of silicalite-1 seed crystals. The scale bars are of 1 μm. (Adopted from Ref. [55] with permission of Publisher)

In addition, the influence of room temperature ageing of the reaction mixture on the product properties has also been investigated. Since in the investigated crystallization system, the seed crystals are added as one of the gradients of the gel precursors, the relevant studies are separated as ageing in the presence or absence of seed crystals.

Figs. 13 and 14 show the SEM images and PSD curves of the ZSM-5 zeolites crystallized from the reaction mixtures aged for different times in the presence of silicalite-1 seed crystals. Although the ageing does not change morphology of the crystals, the particle size distribution becomes narrower with increasing the ageing duration. Moreover, it can also be observed that the particle size of the product slightly decreases with ageing.

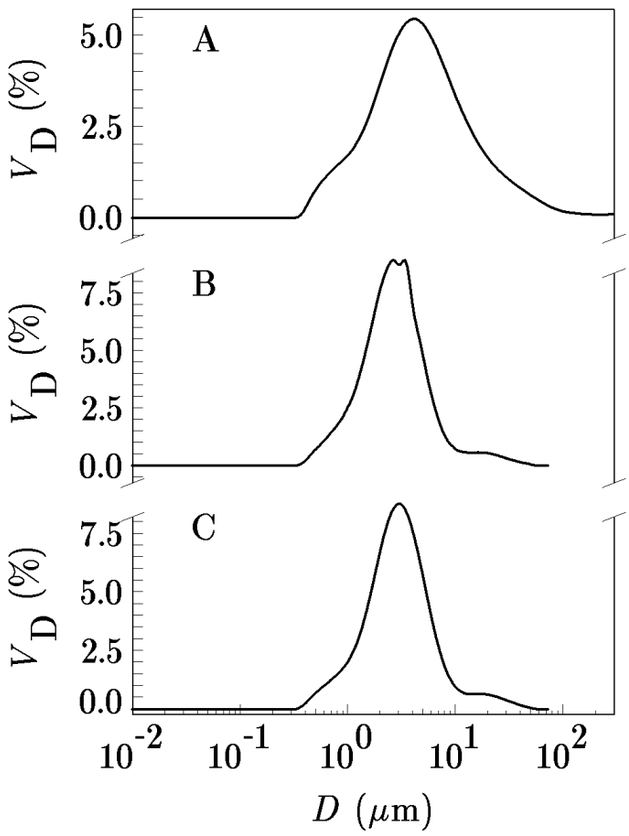

Fig. 14. Particle size distributions by volume of the products obtained by hydrothermal treatment (at 483 K for 2 h) of the reaction mixtures having aged at room temperature for 0 (A), 3 (B) and 48 h (C) in the presence of silicalite-1 seed crystals. (Adopted from Ref. [55] with permission of Publisher)

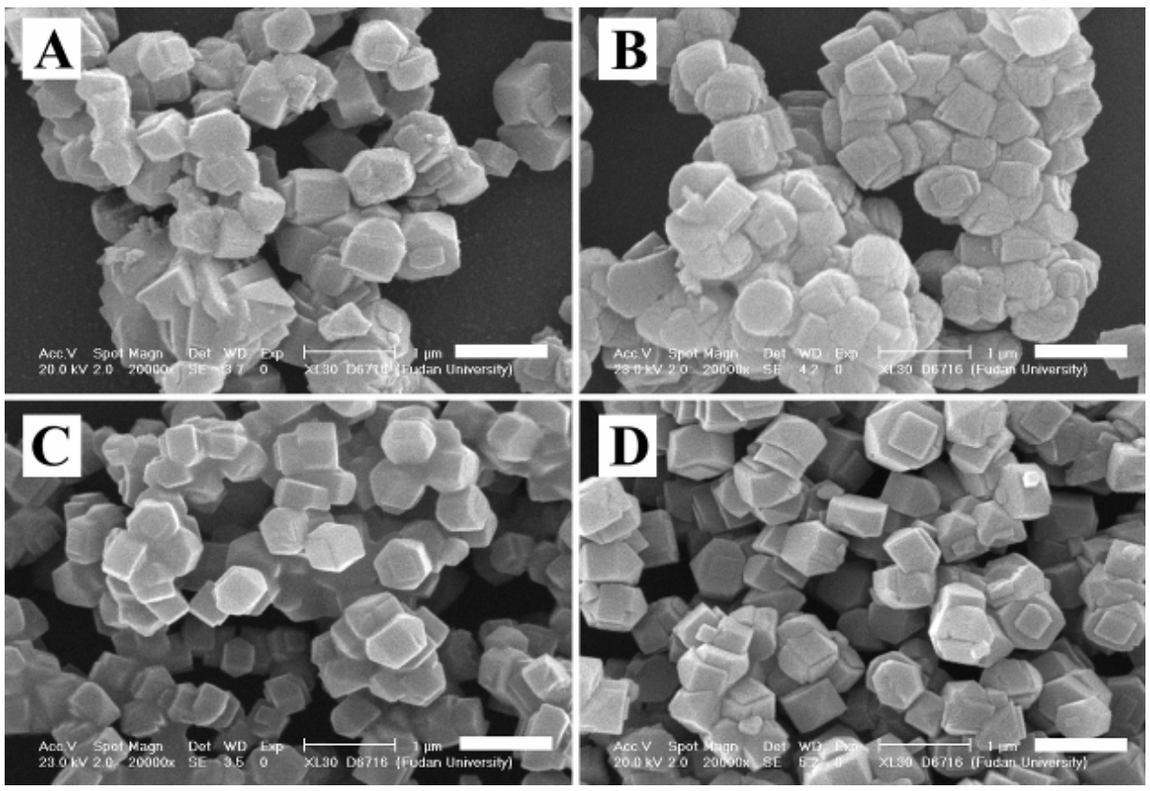

Fig. 15. SEM images of the products obtained by hydrothermal treatment (at 483 K for 2 h) of the reaction mixture (A = 0.008; $[Na^+/SiO_2]_b$ = 0.64) aged at room temperature for 5 (A), 20 (B), 48 (C) and 120 h (D) before addition of seeds and heating. The scale bars are of 1 μm. (Adopted from Ref. [55] with permission of Publisher)

Similar like in the cases of the ageing in the presence of seeds, the results from the ageing of the seed-free reaction mixture also show the same trend (Figs. 15 and 16). The crystallinity of the product does not markedly change with ageing. On the other hand, the PSD curves in Fig. 16 show a gradual decrease of the fraction of large-size "particles" (10 – 500 μm) and simultaneous increase of the fraction of discrete particles (crystals) having the size in the range from 0.45 – 10 μm, with the increase of the ageing duration. This undoubtedly shows that the ageing of the seed-free reaction mixture prevents the agglomeration of growing crystals of zeolite ZSM-5.

The independence of the properties of crystalline end products on the duration of room temperature ageing of reaction mixtures indicates that the formation of precursors for the subsequent growth of ZSM-5 zeolites does not occur during the room-temperature ageing in the current system and, at the same time, this confirms the hypothesis that, under such conditions, the active growth precursors can only be formed at reaction temperature. Since in SDA-free crystallization systems, the formation of new nuclei is greatly suppressed in the presence of seed crystals [51], the size of discrete crystals in the product depend only on the amount and size of the seeds present in the reaction mixture.

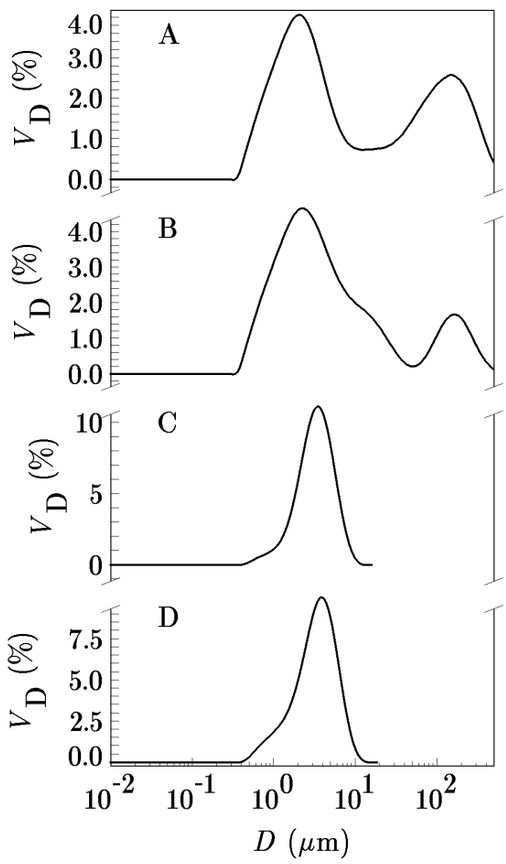

Fig. 16. PSDs by volume of the products obtained by hydrothermal treatment (at 483 K for 2 h) of the reaction mixture (A = 0.008; $[Na^+/SiO_2]_b$ = 0.64) aged at room temperature for 5 (A), 20 (B), 48 (C) and 120 h (D) before addition of seeds and heating. (Adopted from Ref. [55] with permission of Publisher)

On the other hand, the influence of the hydrogel ageing on the PSDs of the crystalline end products is probably connected with the change (increase) of the concentration of Si (most probably in the form of low-molecular weight silicate species) in the liquid phase of the reaction mixture with prolonging ageing duration (Fig. 17). Although the increase of the concentration of Si in the liquid phase during ageing (Fig. 17) does not cause the formation of the growth precursor species at the ageing (room) temperature, it certainly facilitates the formation of the growth precursor species during heating of the reaction mixture, i.e., higher starting concentration of low-molecular weight silicate species causes higher rate of formation of the growth precursor species and thus, higher rate of growth of zeolite ZSM-5 on the silicalite-1 crystals. From this reason, particle (crystal) size at given crystallization time increases with increasing time of hydrogel ageing (Fig. 16). Since, on the other hand (i) crystal growth and agglomeration take place simultaneously and (ii), the rate of agglomeration increases with decreasing particle size [65], tendency of agglomeration decreases with increasing time of hydrogel ageing (Fig. 16).

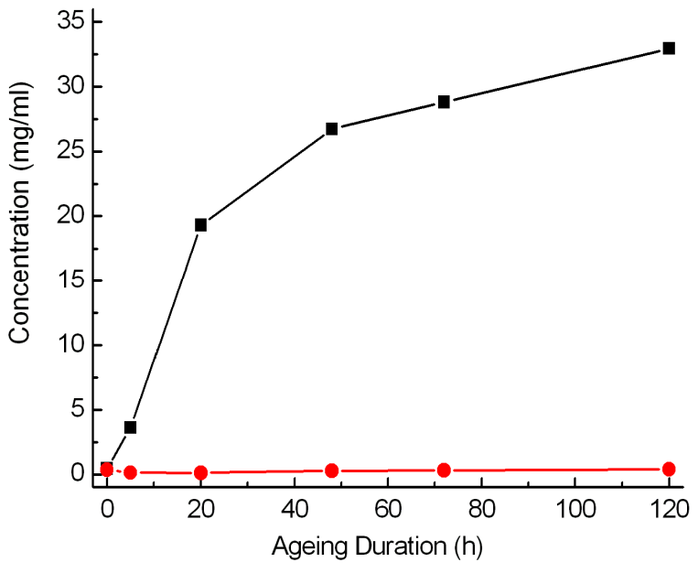

Fig. 17. Influence of the room-temperature ageing of the seed-free reaction mixture (A = 0.008; $[Na+/SiO2]_b$ = 0.64) on: (A) changes in the concentrations of silicon (■) and aluminum (●) in the liquid phase. (Adopted and reproduced from Ref. [55] with permission of Publisher)

5. Crystallization mechanism

With the above studies, the influence of various parameters on the three most important properties (phase purity, particulate properties and chemical composition) of ZSM-5 zeolites can be clearly concluded in Table 2. From this summary, the most pronounced influence is attributed to the batch alkalinity, which changes all the relevant properties of the crystalline-end product. In the large-scale synthesis of ZSM-5 zeolites for application, the batch alkalinity should be strictly controlled to obtain the qualified product. On the other hand, among the mentioned three properties of ZSM-5 zeolites, the particulate properties are most sensitive to the change of the environment of crystallization. Thus, the synthesis of ZSM-5 zeolites with controllable uniform crystal sizes is always a hot, attractive and enduring topic in the field of zeolites.

	Seed size & morphology	Seed amount	Batch alkalinity	Batch sodium ion content	Gel ageing effect
Phase purity (structural property)	-	-	+	-	-
Particulate property (size and distribution)	+	+	+	+	+
Chemical composition (Si/Al in framework)	-	+	+	+/-	-

a. The influences are expressed as pronounced influence (+), less influence (-), and influence depends on the detailed condition

Table 2. Summary of the influences of synthetic parameters on the properties of ZSM-5 product. [a]

The systematic analysis of the parameters governing the crystallization of zeolite ZSM-5 also makes a chance to define the crystallization mechanism of ZSM-5 zeolites in SDA-free system. To achieve the controllable synthesis of ZSM-5 zeolites with designed particulate and chemical properties, the thorough understanding of the critical processes during the crystallization is the only way. Such goal is achieved by both efforts, the kinetic analysis of crystallization processes and the alkaline, post-treatment of final products.

Fig. 18 shows the crystallization curves of the systems containing various amounts (expressed as the weight percentage of silica amount in the batch) of silicalite-1 seed crystals of different sizes. It can be clearly observed that the rate of crystallization considerably depends on both the size and the amount of the added silicalite-1 seed crystals. The time for the completion of crystallization decreases with both decreasing seed size (at constant amount) and increasing amount of seeds (at constant seed size). Furthermore, the crystallization process of the system with 4 wt.% of 260 nm seed crystals was followed by TEM observations (Fig. 19). At the initial stage of crystallization, the seed crystals and amorphous precursors (existing as small particles) can be identified clearly (Fig. 19a). At prolonged hydrothermal treatment, the amorphous precursors start to stack onto the surface of seed crystals and agglomerate together (Figs. 19b and c), followed by depleting of the amorphous precursors and complete ordering of the structure into ZSM-5 crystals (Fig. 19 d). High magnification TEM image (Fig. 20) shows a "core-shell" transformation process of amorphous to crystalline phase (zeolite ZSM-5), which happens at the seed-amorphous interface.

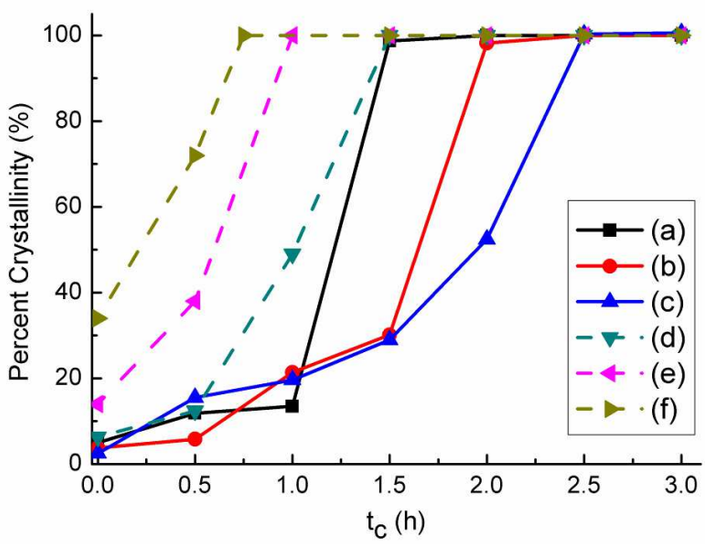

Fig. 18. Crystallization curves of systems with using silicalite-1 seeds of 90 nm-4wt.% (a), 260 nm-4wt.% (b), 690 nm-4wt.% (c), 260 nm-8wt.% (d), 260 nm-16wt.% (e), and 260 nm-32wt.%(f). t_c is the time of crystallization. The percent crystallinity was calculated from the corresponding XRD patterns. (Adopted from Ref. [50] with permission of Publisher)

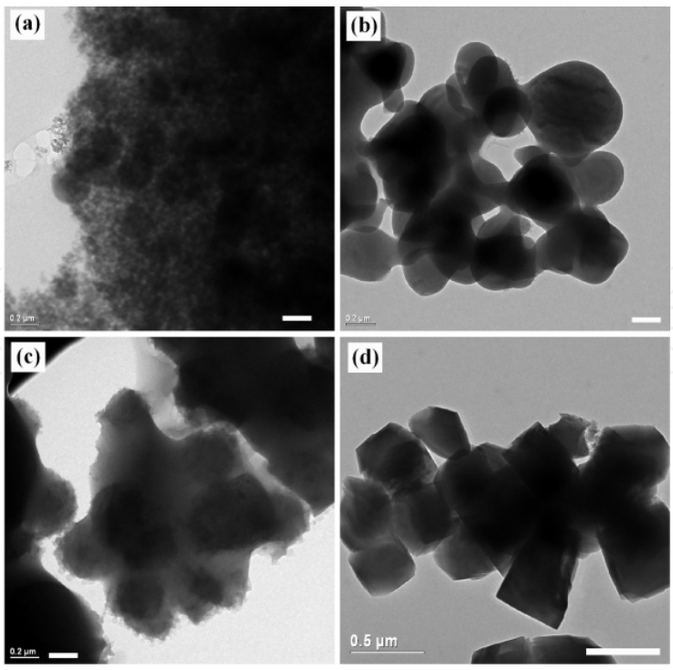

Fig. 19. TEM images of the samples obtained by using 4 wt. % of 260 nm silicalite-1 seed crystals at t_c = 0.5 h (a), t_c = 1.0 h (b), t_c = 1.5 h (c), and t_c = 2.0 h (d). The scale bars in (a), (b), (c), and (d) are of 0.2 µm, 0.2 µm, 0.2 µm, and 0.5 µm, respectively. (Adopted from Ref. [50] with permission of Publisher)

Fig. 21 displays the PSD curves (by number) of the 260 nm silicalite-1 seed crystals (Fig. 21A) and that of the ZSM-5 zeolites obtained using same type of seeds (Fig. 21B). It can be observed that both curves possess almost the same shape and trend. The only difference is the size of crystals. Such phenomenon, although simple, clearly revealed the fact that the total number of crystals during the process of crystallization remains unchanged. It can be deduced that the nucleation process is completely suppressed under the current synthesis condition (SDA-free system with the presence of seed crystals), further proves the only occurrence of the growth of ZSM-5 zeolites on the surface of silicalite-1 seeds.

In addition, the post-synthesis alkaline treatment was carried out on the obtained samples. Since the tetrahedral aluminium centres are relatively inert to hydroxide attack due to the negative charges associated with these centers, and the aluminum atom protects not only the adjacent silicon atoms but also those in the positions of next nearest neighbours [17, 57, 58], it could be expected that, after the alkaline treatment of the final products, the all-silica seed crystals would be dissolved away, leaving behind the aluminium-containing framework of ZSM-5. To check this assumption, the samples are treated with 0.8 M sodium carbonate solution at 80 ^{o}C for 36 h under stirring. Fig. 22 shows the TEM images of the alkaline treated samples. By comparison of untreated and alkaline-treated samples, it can be found that both the size and crystal structure remains unchanged, but the hollow core appears in the centres of particles (crystals) after alkaline treatment. This finding indicates that the crystallization takes place on the surface of seed crystals, which is in accordance with the analysis of the results of kinetic study.

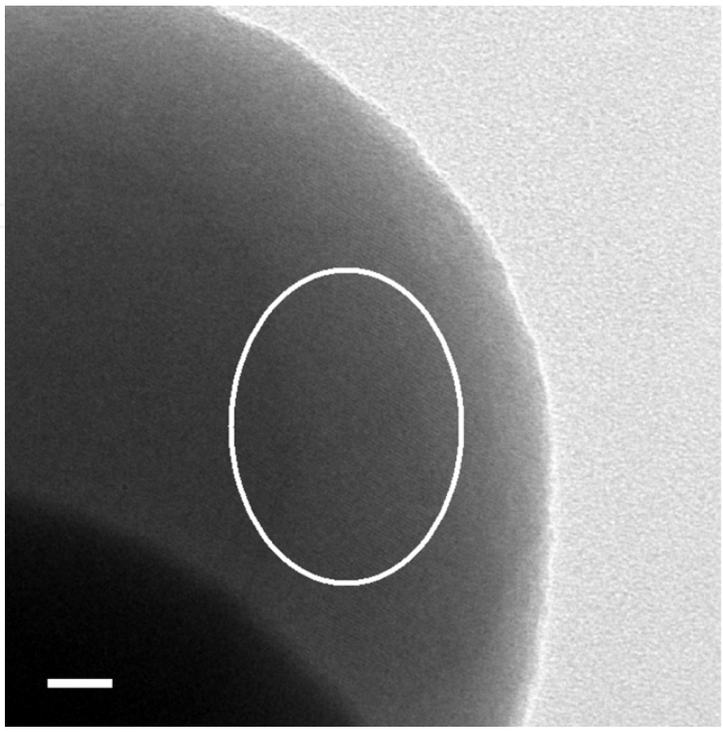

Fig. 20. High magnification TEM image of the sample separated from the reaction mixture containing 4 wt. % of 260 nm silicalite-1 seed crystals at t_c = 1 h. The scale bar is of 20 nm and the crystalline lattice can be identified from the indicated area. (Adopted from Ref. [50] with permission of Publisher)

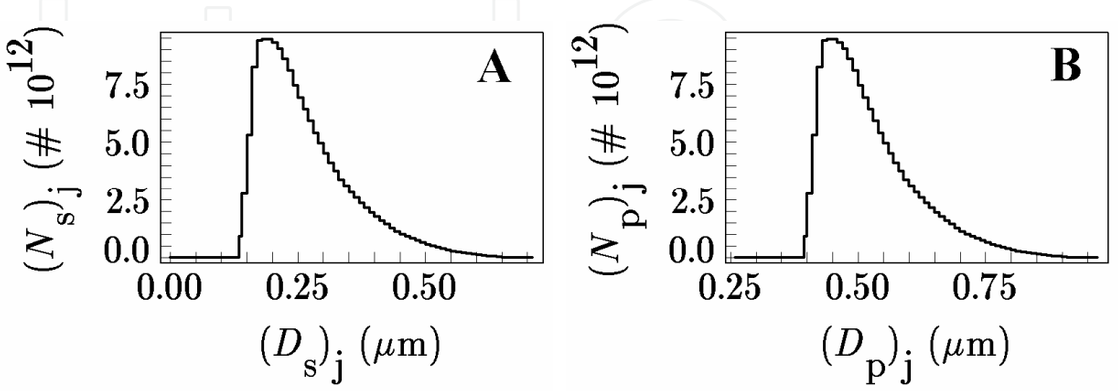

Fig. 21. The PSD curves (by number) of silicalite-1 seed crystals (A) and ZSM-5 product (B) synthesized using 4 wt.%% of the same seed crystals.

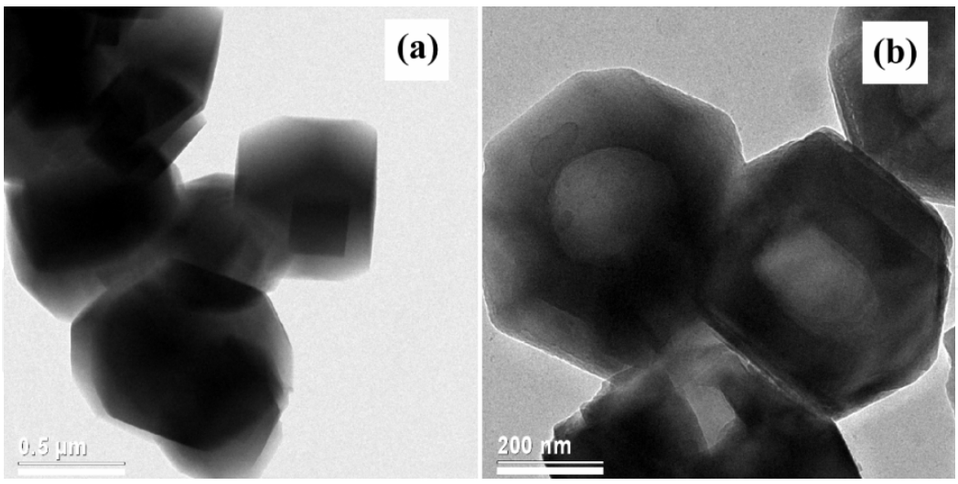

Fig. 22. TEM images of ZSM-5 samples, synthesized from the reaction mixture containing 4 wt. % of 260 nm seed crystals, before (a) and after (b) alkaline treatment. The scale bars in (a) and (b) are of 0.5 µm and 0.2 µm, respectively. (Adopted from Ref. [50] with permission of Publisher)

Taking into consideration of all the relevant mechanistic studies, the crystallization process of SDA-free seed-induced approach can be described as the growth of active species on the surface of seed crystals without formation of new nuclei. All the synthetic parameters influence the properties of the final products by changing either the relative rate or the environment of the growth step during crystallization process.

6. Modeling approach

After the relevant mechanistic studies, the mathematical analysis of the growth step of ZSM-5 zeolites on the surface of silicalite-1 seed crystals becomes possible. Compared with the phenomenological description, the quantitative explanation of the crystallization step makes the further control of the process much easier and convenient. On the basis of above presented data, it can be assumed that the crystallization process is a typical seed-induced one which can be mathematically expressed by a cubic function [50, 59, 60], i.e.

$$m_t = m_0 + K_1 t + K_2 t^2 + K_3 t^3 \quad (1)$$

where m_t is the mass of zeolite crystallized up to the time t and m_0 is the mass of the seed crystals added into the reaction mixture. From the above observations and general knowledge on the crystal growth of zeolites [61], it can be assumed that the crystallization proceeds by a linear, size-independent growth of seed crystals and thus, that the crystal size, d_t, at the crystallization time t, can be expressed as:

$$d_t = d_0 + K_g t \quad (2)$$

where, d_0 represents the size of the seed crystals and K_g is the growth rate constant. Taking into consideration that the formation of nuclei in the crystallizing system is depressed by both by the absence of SDA [50] and presence of seed crystals [50, 59, 60] it is reliable to

assume that the number of growing crystals, N_t, is constant and equal to the number, N_0, of the added seed crystals. Then, the change of the mass, m_t , of the crystallized zeolite ZSM-5 with the crystallization time t, can be expressed as,

$$m_t = G\rho N_t (d_t)^3 = G\rho N_0 (d_0 + K_g t)^3 = G\rho N_0 (d_0)^3 (1 + \frac{K_g}{d_0} t)^3 \tag{3}$$

where, G is the geometrical shape factor of the growing crystals, ρ is the density of crystalline phase (zeolite), and the mass, m_o, of seed crystals can be expressed as:

$$m_0 = G\rho N_0 (d_0)^3 \tag{4}$$

The Eq. (3) can be transformed into

$$m_t = m_0 (1 + \frac{K_g}{d_0} t)^3 = m_0 [1 + 3(\frac{K_g}{d_0})t + 3(\frac{K_g}{d_0})^2 t^2 + (\frac{K_g}{d_0})^3 t^3] \tag{5}$$

where,

$$K_1 = 3(\frac{K_g}{d_0}) m_0 \,,\; K_2 = 3(\frac{K_g}{d_0})^2 m_0 \text{ and } K_3 = (\frac{K_g}{d_0})^3 m_0 \,.$$

Since the total silica-alumina source in the reaction mixture is constant during the synthesis, the values of m_t and m_0 can also be expressed as the fractions x_t and x_0 of aluminosilicate material in the reaction mixture at different crystallization time t. Thus, the Eq. (5) can also be expressed as [59]:

$$x_t = x_0 (1 + \frac{K_g}{d_0} t)^3 \tag{6}$$

where, x_0 is fraction of aluminosilicate material contained in seed crystals at t = 0, and x_t is the fraction of aluminosilicate material in the crystalline phase (seeds + newly crystallized zeolite) at t > 0.

Then, the crystal growth rate constant, K_g, can be obtained by solving the Eq. (6), e.g.,

$$K_g = (\sqrt[3]{\frac{x}{x_0}} - 1) \frac{d_0}{t} \tag{7}$$

Thus, the value of K_g can be calculated by Eq. (7) using d_0 = seed size and x/x_0 = (crystallinity at t/crystallinity at t = 0) (see Fig. 18); K_g = 0.15 μm/h for all investigated system. Then, inserting the calculated value of K_g = 0.15 μm/h and the appropriate values of d_0 = 0.26 μm and x_0 = 1 wt. % into Eq. (5), the kinetics of crystallization of zeolite ZSM-5 from the reaction mixture containing 1 wt. % of 260 nm silicalite-1 seed crystals is calculated (curve in Fig. 23) and compared with the measured kinetics (points in Fig.23). Almost perfect agreement between calculated and measured kinetics indicates that the crystallization process proceeds in expected way, namely by a linear, size-independent growth of silicalite-1 seed crystals.

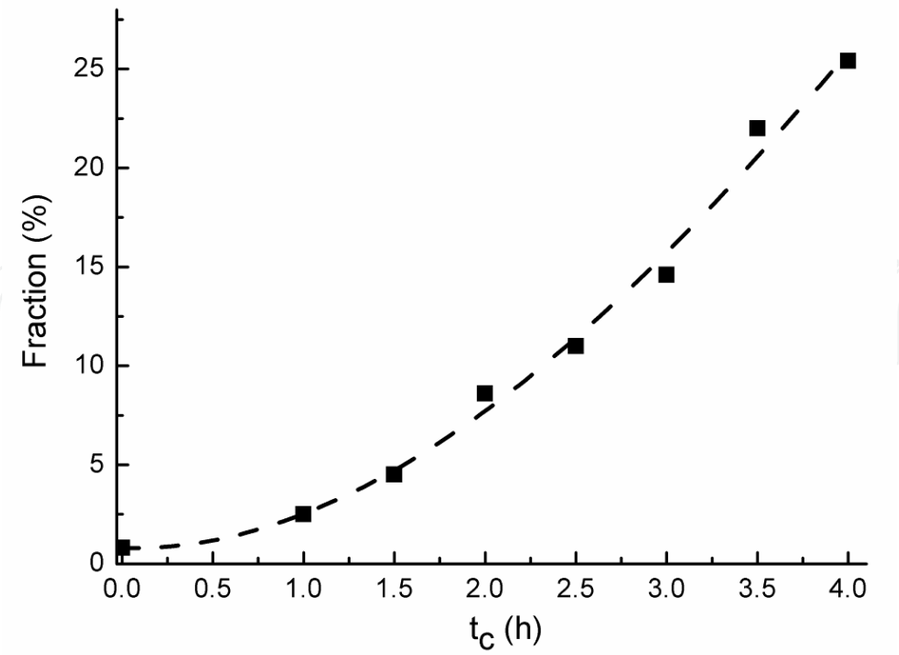

Fig. 23. Correlation between measured kinetics of crystallization of zeolite ZSM-5 from the reaction mixture containing 1 wt. % of 260 nm silicalite-1 seed crystals (points) and the kinetics of crystallization calculated by Eq. (5) (dashed curve). (Adopted from Ref. [50] with permission of Publisher)

On the other hand, an almost perfect correlation can be observed between measured sizes, d_t(det), of the crystalline end products and the corresponding sizes, d_t(cal), calculated by Eq. (2), using the value K_g = 0.15 μm/h, and the corresponding seed sizes, d_0 (Table 3). This phenomenon is an additional evidence to prove that the process of crystallization takes place by the mechanism mathematically described by Eqs. (1) – (6).

d_0 (nm)	Seed addition amount (wt.%)	t_c[a] (h)	d_t(cal)[b] (nm)	d_t(det)[c] (nm)
90	4.0	1.5	315	270
690	4.0	2.5	1065	1100
260	4.0	2.0	560	520
260	8.0	1.5	485	440
260	16.0	1.0	410	410
260	32.0	0.75	373	350

a. determined from the corresponding crystallization curve in Fig. 18 by choosing the first 100% crystallinity data point
b. calculated from Eq. (2) using crystal growth rate of 0.15 μm/h
c. determined from the corresponding SEM images
(Adopted from Ref. [50] with permission of Publisher)

Table 3. The comparison of measured, d_t(det), and calculated, d_t(cal), final crystal sizes of zeolite ZSM-5 synthesized from the reaction mixtures containing different amounts of silicalite-1 seed crystals having different sizes.

Based on the analysis of experimental data in both phenomenological and mathematical way, the crystallization mechanism and the corresponding critical processes occurring during crystallization are depicted in Fig. 24. These processes are: (i) dissolution of amorphous silica and/or alumina sources, (ii) formation of alumino(silicate) gel by poly-condensation reactions and the partial deposition of gel onto the surface of seed crystals, (iii) formation of growth precursor species in the gel matrix at high temperature, (iv) deposition of growth species onto the surface of seed crystals, and (v) final ordering of growth species to form the crystalline end products.

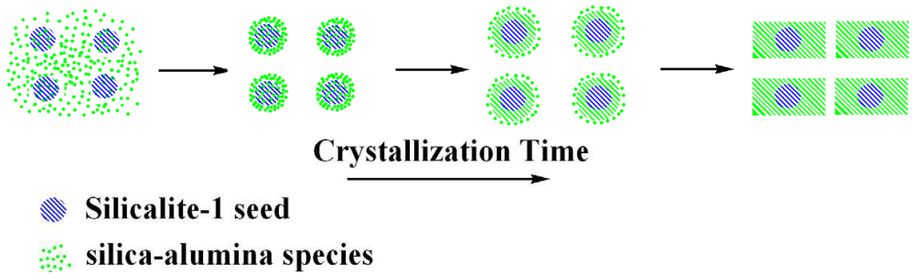

Fig. 24. Schematic presentation of the crystallization process of seed-induced SDA-free approach for the synthesis of sub-micrometer sized ZSM-5 zeolites. (Adopted from [50] with permission of Publisher)

7. Conclusion

In this chapter, the seed-induced, SDA-free crystallization system for the growth of sub-micrometer sized ZSM-5 zeolites is carried out, which clearly shows that:

- The crystallization process is predominantly determined by the growth steps in which the product size and morphologies could be well tuned by the variations of size and amount of silicalite-1 seed crystals;
- The batch alkalinity, expressed as $A = [Na_2O/SiO_2]_b$ plays the key role on the crystallization processes, which influences the phase purity, particulate and chemical composition (Si/Al ratio) of the final product. The optimal alkalinity for growth of pure phase ZSM-5 zeolite is $0.006 \leq A \leq 0.010$;
- The excess batch content of sodium ions and prolonged duration of hydrogel ageing do not enhance the rate of crystallization. Instead, the aggregation behaviour/size uniformity of the products is influenced by these two parameters. This indicates that the precursor species for the growth of ZSM-5 are generated at high temperature controlled by batch alkalinity, rather than by the concentration of sodium ions at room temperature;
- The crystallization mechanism of the seed-induction SDA-free approach is revealed as the typical size-independent, linear growth process on the seed surface.

With the understanding of the critical processes occurring during the crystallization of ZSM-5 zeolites, it is expected that the ZSM-5 zeolites possessing more interesting properties could be obtained by the co-ordinately variation of multi-synthesis parameters at the same time. This work will also make corresponding contributions on the rational design of ZSM-5 zeolites with desired functionalities in the domain of both materials and industrial catalysis.

8. Acknowledgement

This work is realized in the frame of the projects: NSFC (20803010), "Chen Guang" project supported by Shanghai Municipal Education Commission and Shanghai Education Development Foundation (09CG02), 'Brain Gain' Post-Doc project (I-668-2011) supported by Croatian Science Foundation and the project 098-0982904-2953, financially supported by the Ministry of Science, Education and Sport of the Republic of Croatia.

9. References

[1] Argauer , R. J.; Landolt, G. R., Mobile Oil, US Patent 3, 702, 886, 1972.
[2] Singh, R.; Dutta, P. K., 'MFI: A Case Study of Zeolite Synthesis', in Auerbach, S.M.; Carrado, K.A.; Dutta, P.K. Eds. *Handbook of Zeolite Science and Technology*, Chapter 2, Marcel Dekker Inc, New York-Basel, 2003, p21.
[3] Adewuyi, Y.G.; Klocke, D.J.; Buchnan, J.S. *Appl. Catal. A-General* 1995, *131*, 121.
[4] Chen, N.Y.; Garwood, W.E.; Dwyer, F.G. *Shape Selective Catalysis in Industrial Applications*, 2nd edition, Marcel Dekker Inc., New York, 1996.
[5] Kim, S.D.; Noh, S.H.; Park, J.W.; Kim, W.j. *Microporous Mesoporous Mater*. 2006, *92*, 181.
[6] Narita, E.; Sato, K.; Okabe, T. *Chem. Lett.* 1984, 1055.
[7] Jacobs, P. A.; Martens, J. A., *Stud. Surf. Sci. Catal.* 1987, *33*, 1.
[8] Weitkamp, J. *Solid State Ionics* 2000, *131*, 175.
[9] Vedrine, J.C. *ACS Symp. Ser.* 1985, *297*, 257.
[10] Renzo, F.D. *Catal. Today* 1998, *41*, 37.
[11] Chao, K.-J.; Tsai, T.C.; Chen, M.-S. *J. Chem. Soc. Faraday Trans*. 1981, *77*, 547.
[12] Romannikov, V.N.; Mastikhin, V.M.; Hočevar, S.; Držaj, B. *Zeolites* 1983, *3*, 310.
[13] Gabelica, Z.; Derouane, E.G.; Blom, N. *Adv. Chem. Ser.* 1984, *248*, 219.
[14] Padovan, M.; Leofanti, G.; Solari, M.; Moretti, E. *Zeolites* 1984, *4*, 295.
[15] Scholle, K.F.M.G.J.; Veeman, W.S.; Frenken, P.; van der Velden, G.P.M. *Catal. Today* 1985, *17*, 233.
[16] Gabelica, Z., Nagy, J.B.; Debras, G.; Derouane, E.G. *Acta Chimica Hungarica* 1985, *119*, 275.
[17] Čižmek, A.; Subotić, B.; Aiello, R.; Crea, F.; Nastro, A.; Tuoto, C. *Microporous Mater.* 1995, *4*, 159.
[18] Cundy, C.S.; Henty, M.S.; Plaisted, R.J. *Zeolites* 1995, *15*, 353.
[19] Erdem, A.; Sand, L.B. *J. Catal.* 1979, *60*, 241.
[20] Derouane, E.G.; Detremmerie, S.; Gabelica. Z.; Blom, N. *Appl. Catal.* 1981, *1*, 201.
[21] Mostowicz, R.; Sand, L.B. *Zeolites* 1983, *3*, 219.
[22] Gabelica, Z.; Blom, N.; Derouane, E.G. *Appl. Catal.* 1983, *5*, 227.
[23] Nastro, A.; Sand, L.B. *Zeolites* 1983, *3*, 57.
[24] Nastro, A.; Aiello, R.; Colella, C. *Ann. Chim.* 1984, *74*, 579.
[25] Ghamami, M.; Sand, L.B. *Zeolites* 1983, *3*, 155.
[26] Chang, C.D.; Lang, W.H.; Silvestri, A.J. US Patent 3 894 106, 1975.
[27] Pan, M.; Lin, J.S. *Microporous Mesoporous Mater.* 2001, *43*, 319.
[28] Dokter, W.H.; van Garderen, H.F.; Beleen, T.P.M.; van Santen, R.A.; Bras, V. *Angew. Chem. Int. Ed. Engl.* 1995, *34*, 73.
[29] Subotic, B.; Bronic, J.; Jelic, T. A. in *Ordered Porous Solids*, Elsevier B.V. 2009, Chapter 6.
[30] Persson, A.E.; Schoeman, B. J.; Sterte, J.; Otterstedt, J.E. *Zeolites* 1995, *15*, 611.
[31] Hsu, C.Y.; Chiang, A.S.T.; Selvin, R.; Thompson, R.W. *J. Phys. Chem. B* 2005, *109*, 18804.
[32] Geus, E.R.; van Bekkum, H. *Zeolites* 1995, *15*, 333.
[33] Lin, X.; Falconer, J.L. Noble, R.D. *Chem. Mater.* 1998, *10*, 3716.

[34] Lai, R. ; Gavalas, G.R. *Microporous Mesoporous Mater.* 2000, *38*, 239.
[35] Lassinatti, M.; Jereman, F.; Hedlund, J.; Creaser, D.; Sterte, J. *Catal. Today* 2001, *67*, 109.
[36] Kalipcilar, H.; Culfaz, A. *Cryst. Res. Technol.* 2001, *36*, 1197.
[37] Grose, R.W.; Flanigen, E.M US Patent 4 257 885, 1981.
[38] Narita, E.; Sato, K.; Yatabe, N.; Okabe, T. *Ind. Eng. Chem. Prod. Res. Dev.* 1985, *24*, 507.
[39] Berak, J.M.; Mostowicz, R. *Stud. Surf. Sci. Catal.* 1985, *24*, 47.
[40] Batista, J.; Kaučič, V. Vestn. *Slov. Kem. Drus.* 1987, *34*, 289.
[41] Aiello, R.; Crea, F.; Nastro, A.; Pellegrino, A. *Zeolites* 1987, *7*, 549.
[42] Dai, F.-Y.; Suzuki, M.; Takahashi, H.; Y. Saito, *ACS Sym. Ser.* 1989, *398*, 224.
[43] Schweiger, W.; Bergk, K.-H.; Freude, D.; Hunger, M.; Pfeifer, H. *ACS Sym. Ser.* 1989, *398*, 274.
[44] Nastro, A.; Crea, F.; Hayhurst, D.T.; Testa, F.; Aiello, R.; Toniolo, L. *Stud. Surf. Sci. Catal.* 1989, *49A*, 321.
[45] Mravec, D.; Riečanova, D.; Ilavsky, J.; Majing, *J. Chem. Papers* 1991, *45*, 27.
[46] Lowe, B. M.; Nee, J.R.D.; Casci, J.L. *Zeolites* 1994, *14*, 610.
[47] Otake, M. *Zeolites* 1994, *14*, 42.
[48] Cheng, Y.; Wang, L.J.; Li, J.S.; Yang, Y.C.; Sun, X.Y. *Mater. Lett.* 2005, *59*, 3427.
[49] Cheng, Y.; Liao, R.H.; Li, J.S.; Sun, X.Y.; Wang, L.J. J. *Mater. Process. Technol.* 2008, *206*, 445.
[50] Ren, N.; Yang, Z.J.; Lv, X.C.; Shi, J.; Zhang, Y.H.; Tang, Y. *Micropor. Mesopor. Mater.* 2010, *131*, 103.
[51] Gonthier, S.; Thompson, R.W. *Stud. Surf. Sci. Catal.* 1994, *85*, 43.
[52] Majano, G.; Delmotte, L.; Valtchev, V.; Mintova, S. *Chem. Mater.* 2009, *21*, 4184.
[53] Cundy, C.S.; Plaisted, R.J.; Zhao, J.P. *Chem. Commun.* 1998, 1465.
[54] Ren, N.; Bronić J.; Subotić, B.; Lv, X.C.; Yang, Z.J.; Tang, Y. *Microporous Mesoporous Mater.* 2011, *139*, 197.
[55] Ren, N.; Bronić J.; Subotić, B.; Song, Y.M.; Lv, X.C.; Tang, Y. *Microporous Mesoporous Mater.* 2012, *147*, 229.
[56] Derouane, E.G.; Gabelica, Z. *J. Solid State Chem.* 1986, *64*, 296.
[57] Nastro, A.; Gabelica, Z.; Bodart, P.; Nagy J. B. in: Kaliaguine, S.; Mahay, A. (Eds.), *Catalysis on the Energy Scene*, Elsevier Science Publishers B.V., Amstardam, 1984, p. 131.
[58] Nagy, J.B.; Bodart, P.; Collette, H.; Fernandez, C.; Gabelica, Z.; Nastro, A.; Aiello, R. *J. Chem. Soc. Faraday Trans. I* 1989, *85*, 2749.
[59] Čižmek, A.; Subotić, B.; Kralj, D.; Babić-Ivančić, V.; Tonejc, A. *Microporous Mater.* 1997, *12*, 267.
[60] Zhdanov, S.P.; Samulevich, N.N. in: L.V. Rees (Ed.), Proceedings of the Fifth International Conference on Zeolites, Heyden, London, Philadelphia, Rheine, 1980, p. 75.
[61] Larlus, O.; Valthev, V.P. *Chem. Mater.* 2004, *16*, 3381.
[62] Zhu, G. ; Li, Y. ; Chen, H. ; Liu, J. ; Yang, W. *J. Mater. Sci.* 2008, *43*, 3279.
[63] Kang, N.Y. ; Song, B.S. ; Lee, C.W. ; Choi, W.C. ; Yoon, K.B. ; Park, Y.K. *Microporous Mesoporous Mater.* 2009, *118*, 361.
[64] Iller, R.K. *The Chemistry of Silica*, Willey, New York, 1979.
[65] Kawashima, Y.; Capes, C.E. *Powder Technology*, 1976, *13*, 279.
[57] Lechert, H.; Kacirek, H. *Zeolites* 1991, *11*, 720.
[58] Dessau, R. M.; Valyocsik, E. W.; Goeke, N. H. *Zeolites* 1992, *12*, 776.
[59] Kacirek, H.;. Lechert, H. *J. Phys. Chem.* 1975, *79*, 1589.
[60] Grujic, E.; Subotic, B.; Despotovic, L.J.A. *Stud. Surf. Sci. Catal.* 1989, *49A*, 261.
[61] Subotić, B.; Bronić, J. in: S.M. Auerbach, K.A. Carrado and P.K. Dutta (Eds.), *Handbook of Zeolite Science and Technology*, Marcel Dekker Inc., New York – Basel, 2003, p. 129.

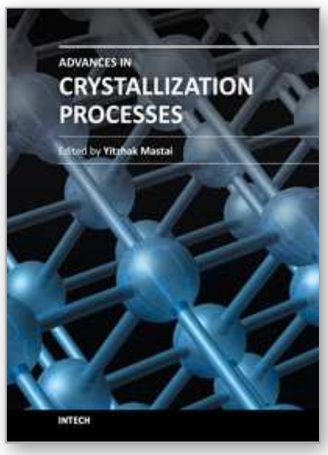

Advances in Crystallization Processes
Edited by Dr. Yitzhak Mastai

ISBN 978-953-51-0581-7
Hard cover, 648 pages
Publisher InTech
Published online 27, April, 2012
Published in print edition April, 2012

Crystallization is used at some stage in nearly all process industries as a method of production, purification or recovery of solid materials. In recent years, a number of new applications have also come to rely on crystallization processes such as the crystallization of nano and amorphous materials. The articles for this book have been contributed by the most respected researchers in this area and cover the frontier areas of research and developments in crystallization processes. Divided into five parts this book provides the latest research developments in many aspects of crystallization including: chiral crystallization, crystallization of nanomaterials and the crystallization of amorphous and glassy materials. This book is of interest to both fundamental research and also to practicing scientists and will prove invaluable to all chemical engineers and industrial chemists in the process industries as well as crystallization workers and students in industry and academia.

How to reference
In order to correctly reference this scholarly work, feel free to copy and paste the following:

Nan Ren, Boris Subotić and Josip Bronić (2012). Crystallization of Sub-Micrometer Sized ZSM-5 Zeolites in SDA-Free Systems, Advances in Crystallization Processes, Dr. Yitzhak Mastai (Ed.), ISBN: 978-953-51-0581-7, InTech, Available from: http://www.intechopen.com/books/advances-in-crystallization-processes/crystallization-of-sub-micron-meter-sized-zsm-5-zeolites-in-sda-free-system

INTECH
open science | open minds

InTech Europe
University Campus STeP Ri
Slavka Krautzeka 83/A
51000 Rijeka, Croatia
Phone: +385 (51) 770 447
Fax: +385 (51) 686 166
www.intechopen.com

InTech China
Unit 405, Office Block, Hotel Equatorial Shanghai
No.65, Yan An Road (West), Shanghai, 200040, China
中国上海市延安西路65号上海国际贵都大饭店办公楼405单元
Phone: +86-21-62489820
Fax: +86-21-62489821

© 2012 The Author(s). Licensee IntechOpen. This is an open access article distributed under the terms of the Creative Commons Attribution 3.0 License, which permits unrestricted use, distribution, and reproduction in any medium, provided the original work is properly cited.

IntechOpen

IntechOpen